Fracture phenomena of disordered media

Chung, Jim

2

FRACTURE OF DISORDERED THREE-DIMENSIONAL SPRING NETWORKS: A COMPUTER SIMULATION METHODOLOGY

2.1 INTRODUCTION

This chapter concentrates on a methodology that is aimed at finding a relation between the mechanical strength of porous media and its microstructural features. The microstructure of a typical highly porous ceramic material is depicted in Figure 2.1.

The geometrical inhomogeneity of the microstructure makes the fracturing process particularly complicated because it is very sensitive to local crack formation. These local cracks can be the starting point of global failure. The modeling takes place at the length scale of the individual pores (typically ~100 nm, but this can be controlled to a certain extent by adjusting manufacturing parameters). The porous material is modeled as a three-dimensional, geometrically inhomogeneous network of spheres or nodes, connected by springs or beams.

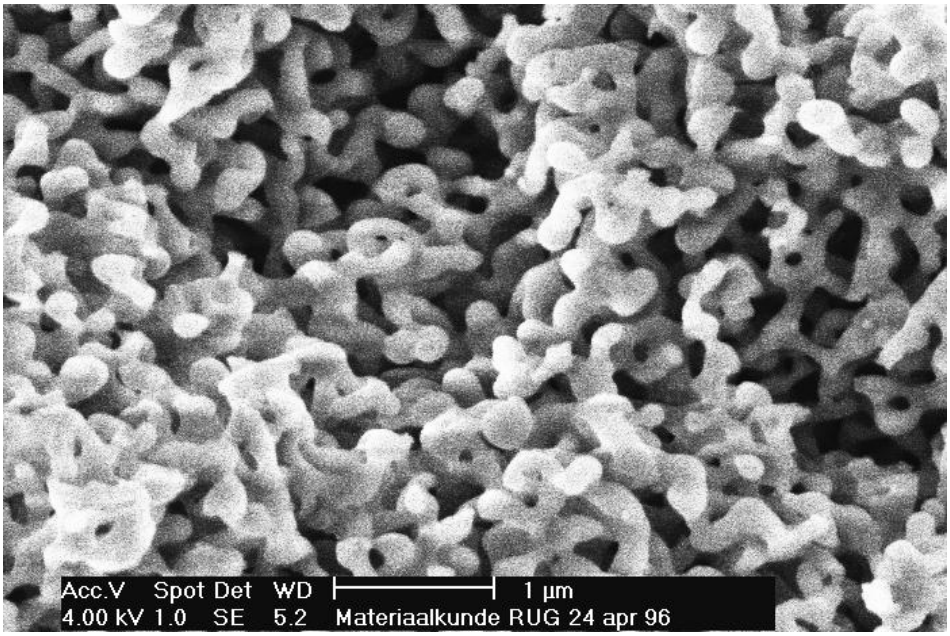

Figure 2.1. Typical microstructure of a SiO_2 extrudate

Elastic networks of springs or beams are frequently used to model the relation between mechanical properties of materials and their microstructure. Simulations have been carried out both in two[1,2,3,4] and three [1,4,5,6,7] dimensions, mainly on regular spring networks. In these simulations, a network is loaded by an external force or displacement, after which some potential function of the nodal displacements is minimized. Mechanical properties can be studied from the resulting equilibrium configuration.

The general field of application of this work lies in the area of catalyst carriers, where highly porous ceramic materials (60-70 vol. %) are commonly used. Due to their large internal surface (up to 250 m^2/g), they are well suited as catalyst carriers for chemical processes (See for example Figure 2.1, where the microstructure of a SiO_2 extrudate is shown).[1,8] The catalyst carriers exhibit brittle fracture behavior and when used in a reactor, they may fail due to their own weight. Crumbled catalyst carriers can block the diffusion paths of reactants through the material. Furthermore, the flow of reactants can move the debris out of the reactor, thereby reducing the reactive area. For that reason, the focal point of the methodology is to obtain a physical description of the ultimate strength in conjunction with its size dependence. Experimentally, this is accessible through the side crushing strength, SCS, also known as the Brazilian

test [1,8] which is believed to measure indirectly the tensile strength. In this chapter, the emphasis is on the methodology as such, whereas size-dependence will be reported in chapter 4.

2.2 COMPUTATIONAL PROCEDURE

The computational procedure consists of various independent steps. The first step is the generation of a network in which a disordered configuration of spheres. After that the central points of the spheres are used as points for connecting the springs (see Chapter 7). The next step consists of a sequence of applying a force and calculating the corresponding displacements and subsequently imposing fracture criteria. This sequence is repeated until the network falls apart into two or more pieces.

Initially, a number of spheres N are arranged on a simple cubic lattice. The spheres are given a Maxwell-Boltzmann velocity distribution at a certain temperature T. A molecular dynamics (MD) run is carried out[9] using a Lennard-Jones potential to obtain a disordered configuration.

When the system is equilibrated, spatial configurations of the system will be sampled. In each of the sampled configurations, the center positions of the spheres will serve as node positions. All nodes are connected if they are within a predefined connecting distance, the *connectivity threshold* C_0, from each other. This is the initial stress free model for the geometry in Figure 2.2.

The top surface is defined as the set of spheres lying within some pre-set vertical distance from the sphere with the largest z coordinate. The bottom surface is defined analogously. The external force is applied at the top and bottom surfaces of the network. The total force on the top surface is equal in magnitude but opposite in direction to the total force on the bottom surface. The other surfaces are not constrained, and so the network is free to expand in the horizontal directions, conform the configuration in the SCS.

A brittle material can only withstand small deformations. This is captured in the model by imposing a fracture criterion on the bonds. If a bond is stretched or compressed beyond a pre-set value, or if a bond or torsion angle change

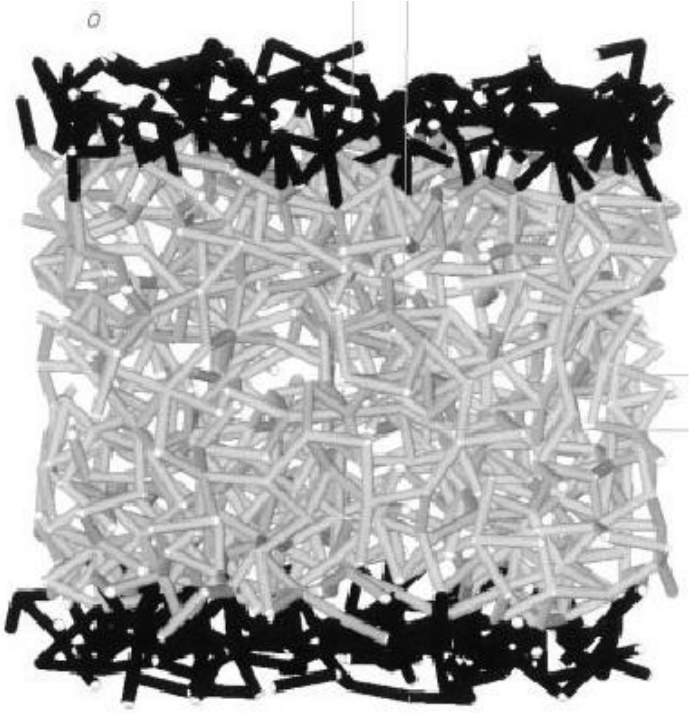

Figure 2.2. A geometrically disordered, three-dimensional network (1000 nodes). Blue bonds are connected to nodes in the top or bottom layers. For colors see Chapter 7.

exceeds a certain threshold, the bond is irreversibly removed from the network. The local stress has to be redistributed through the remaining bonds, leading to a new equilibrium configuration.

Other bonds or angles that now fulfill the fracture criteria are removed from the network. Brittle fracture of the bonds is modeled by allowing only small length and angular changes. This also ensures that the elastic behavior remains linear in terms of the nodal displacements.

By increasing the external stress, this process eventually leads to global failure. The step size at which the force increases should be large enough to limit the time of the total simulation. On the other hand, if the step is too large, too many bonds will break in one step, which makes it difficult to monitor crack

formation and propagation. The system is in equilibrium for given internal and external stresses when a minimum in the total energy is reached.

The total elastic energy consists of a two-body *central force (CF)*, a three-body *bond-bending (BB)* and a four-body *torsion (T)* contribution:

$$U_{EL} = U_{CF} + U_{BB} + U_T \tag{2.1}$$

In the new equilibrium configuration, the fracture criteria can be applied. In the present model, three fracture criteria are adopted: one for stretching, one for bond angle change, and one for torsion angle change. The elongation and compression criterion is fulfilled when the strain of a bond is larger than a pre-set value Δ_{CF}. In that case, the bond is removed from the network. Similarly, if the change in bond angle exceeds a threshold Δ_{BB}, the bond with the largest change in bond angle from its unloaded equilibrium position is removed. Finally, a threshold Δ_T is imposed on the torsion angle per unit length, beyond which the bond is removed. The values of Δ_{CF}, Δ_{BB}, and Δ_T do not necessarily have to be the same for all bonds, but can be distributed over the network according to some probability distribution,[4] thus mimicking possible inhomogeneities in the yield strength of the material on the pore size scale. Brittleness is mimicked by choosing small (~1%) threshold values. When some bonds have been removed, the stress has to redistribute itself along the remaining bonds. The external stress may also change. Under these conditions, the equilibrium configuration changes and so the procedure described above has to be iterated. After a number of increments, so many bonds have broken that there is no longer a percolating cluster of bonds: the system has fallen apart into two (or more) pieces.

In this work, linear elasticity and small displacements of the spheres are assumed, so the displacements enter quadratically in the potential energy. This is ensured by the afore-mentioned choice of brittle fracture criteria. In the following the description of the potential is given in a concise way (convention: $\mathbf{A}$ is a vector in R^3, with components A^q (q ϵ {x,y,z}) and length $|\mathbf{A}| \equiv \sqrt{(A^x)^2 + (A^y)^2 + (A^z)^2}$. Also, $\hat{A} \equiv A/|A|$)

The central force (CF) contribution consists of a Hookean spring potential:

$$U_{CF}(n+1) = \frac{1}{2}\sum_{<ij>} k_{ij}^{CF}[\left|\vec{R}_{ij}(n+1)\right| - \left|\vec{R}_{ij}(0)\right|]^2$$
$$\approx \frac{1}{2}\sum_{<ij>} k_{ij}^{CF}[\Delta\vec{u}_{ij}(n+1)\cdot\hat{R}_{ij}(n) + (\left|\vec{R}_{ij}(n)\right| - \left|\vec{R}_{ij}(0)\right|)]^2, \quad (2.2)$$

where the summation is over all <*ij*> pairs of connected neighbors. The bond vector $\vec{R}_{ij}(n)$ from node *i* to node *j* (≡ bond *i j*) at increment *n* is defined as $\vec{r}_j(n) - \vec{r}_i(n)$, where $\vec{r}_i(n)$ is the position vector of node *i* at increment *n*. Furthermore, the displacement increment $\Delta\vec{u}_{ij}(n)$ at increment *n* is given by $\Delta\vec{u}_j(n) - \Delta\vec{u}_i(n)$, with $\Delta\vec{u}_i(n) \equiv \vec{u}_i(n+1) - \vec{u}_i(n)$ the displacement increment of node *i* and $\vec{u}_i(n) \equiv \vec{r}_i(n) - \vec{r}_i(0)$ the displacement of node *i* at increment *n*. The force constant k_{ij}^{CF} of bond *ij* (the *CF-constant*) is written as

$$k_{ij}^{CF} = \frac{A_{ij}E_{ij}}{\left|\vec{R}_{ij}(0)\right|}, \quad (2.3)$$

with A_{ij} the cross-sectional area of bond *ij* (all cross sections are assumed to be circular) and E_{ij} its Young's modulus.

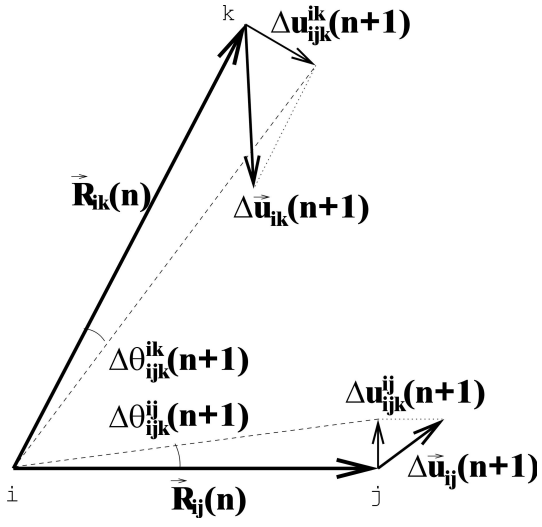

Figure 2.3. Three-body potential.

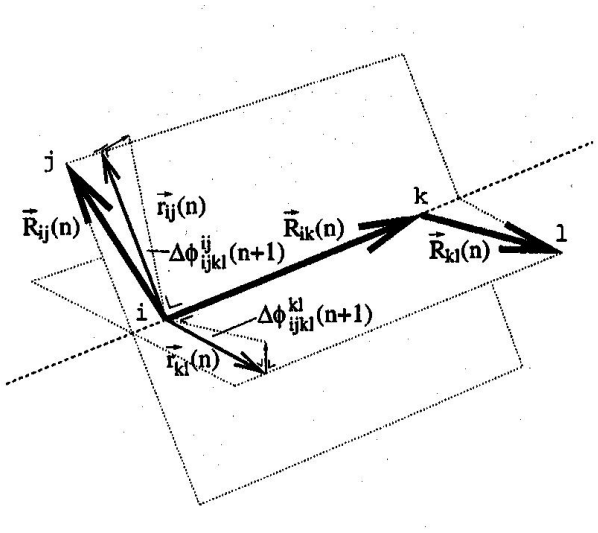

Figure 2.4. Torsion potential

For the bond-bending potential term, consider triplets of spheres *i*, *j*, and *k*, with *j* and *k* at a distance less than C_0 of the central sphere *i* (Figure 2.3). The relevant term is $\theta_{ijk}(n)$, the total *change* of bond angle between bonds *ij* and *ik* at increment *n*, relative to the initial bond angle [i.e., $\theta_{ijk}(0) \equiv 0$]. The bond angle increment $\Delta\theta_{ijk}(n+1) \equiv \theta_{ijk}(n+1) - \theta_{ijk}(n)$ can be split into $\Delta\theta^{ij}_{ijk}(n+1)$, the bond angle change due to $\Delta\vec{u}_{ij}(n+1)$ only, keeping $\vec{R}_{ik}$ fixed, and $\Delta\theta^{ik}_{ijk}(n+1)$, defined analogously:

$$\Delta\theta_{ijk}(n+1) = \Delta\theta^{ij}_{ijk}(n+1) + \Delta\theta^{ik}_{ijk}(n+1) \tag{2.4}$$

The bond-bending potential is given by

$$U_{BB}(n+1) = \frac{1}{2}\sum_{<ijk>} k^{BB}_{ijk}\theta^2_{ijk}(n+1) = \frac{1}{2}\sum_{<ijk>} k^{BB}_{ijk}[\Delta\theta^{ij}_{ijk}(n+1) + \Delta\theta^{ik}_{ijk}(n+1) + \theta_{ijk}(n)]^2, \tag{2.5}$$

where the summation is over all <*ijk*> triplets as in Figure 2.3. $k^{BB}_{ijk}[Nm]$ is the three-body force constant (the *BB-constant*) between nodes *i*, *j*, and *k*. The (small) change in bond angle $\Delta\theta_{ijk}(n+1)$ is related to the component of the displacements $\Delta\vec{u}_{ij}(n+1)$ and $\Delta\vec{u}_{ik}(n+1)$ in the plane defined by spheres *i*, *j*, *k*, in the direction orthogonal to $\vec{R}_{ij}(n)$ and $\vec{R}_{ik}(n)$, respectively. The components of

the displacements $\Delta u_{ij}^{ijk}(n+1)$ and $\Delta u_{ik}^{ijk}(n+1)$ in the *i*, *j*, *k*, plane in these directions become (a slightly different approach can be found in Wang[6]):

$$\Delta\vec{u}_{ij}(n+1)\cdot\left(\frac{[\vec{R}_{ik}(n)\times\vec{R}_{ij}(n)]\times\vec{R}_{ij}(n)}{\left|[\vec{R}_{ik}(n)\times\vec{R}_{ij}(n)]\times\vec{R}_{ij}(n)\right|}\right)\equiv\Delta u_{ij}^{ijk}(n+1) \tag{2.6}$$

and

$$\Delta\vec{u}_{ik}(n+1)\cdot\left(\frac{[\vec{R}_{ij}(n)\times\vec{R}_{ik}(n)]\times\vec{R}_{ik}(n)}{\left|[\vec{R}_{ij}(n)\times\vec{R}_{ik}(n)]\times\vec{R}_{ik}(n)\right|}\right)\equiv\Delta u_{ik}^{ijk}(n+1). \tag{2.7}$$

For small changes in bond angle, the following approximation can be made:

$$\Delta\theta_{ijk}(n+1)\approx\tan[\Delta\theta_{ijk}^{ij}(n+1)]+\tan[\Delta\theta_{ijk}^{ik}(n+1)]=\frac{\Delta u_{ij}^{ijk}(n+1)}{\left|\vec{R}_{ij}(n)\right|}+\frac{\Delta u_{ik}^{ijk}(n+1)}{\left|\vec{R}_{ik}(n)\right|}, \tag{2.8}$$

so that $\Delta\theta_{ijk}^{ij}(n+1)$ and $\Delta\theta_{ijk}^{ik}(n+1)$ can be written as

$$\Delta\theta_{ijk}^{ij}(n+1)=\Delta\vec{u}_{ij}(n+1)\cdot\left(\frac{[\hat{R}_{ik}(n)\times\hat{R}_{ij}(n)]\hat{R}_{ij}(n)-\hat{R}_{ik}(n)}{\left|\vec{R}_{ij}(n)\right|\sqrt{1-[\hat{R}_{ij}(n)\cdot\hat{R}_{ik}(n)]^2}}\right)\equiv\Delta\vec{u}_{ij}(n+1)\cdot\vec{B}_j, \tag{2.9}$$

$$\Delta\theta_{ijk}^{ik}(n+1)=\Delta\vec{u}_{ik}(n+1)\cdot\left(\frac{[\hat{R}_{ij}(n)\times\hat{R}_{ik}(n)]\hat{R}_{ik}(n)-\hat{R}_{ik}(n)}{\left|\vec{R}_{ik}(n)\right|\sqrt{1-[\hat{R}_{ij}(n)\cdot\hat{R}_{ik}(n)]^2}}\right)\equiv\Delta\vec{u}_{ik}(n+1)\cdot\vec{B}_k. \tag{2.10}$$

Furthermore, $\theta_{ijk}(n)$ is given by

$$\Delta\theta_{ijk}(n+1)=\cos^{-1}[\hat{R}_{ij}(n)\times\hat{R}_{ik}(n)]-\cos^{-1}[\hat{R}_{ij}(0)\times\hat{R}_{ik}(0)]. \tag{2.11}$$

The restoring force is modeled as originating from sphere *i*, which acts as a hinge. In order to find a reasonable expression for the *BB* force constant for this

hinge, an analogy is drawn with the theory of bending beams. From elasticity theory,[10] the force constant for a bending beam *ij* is given by (with I_{ij} [m^4] the second moment of area of bond *ij*):

$$k_{ijk}^{ij,BB} = \frac{3E_{ij}I_{ij}}{\left|\vec{R}_{ij}(n)\right|} \tag{2.12}$$

and analogously for bond *ik*. Equating the torques acting on the *ijk* system in equilibrium yields an expression for the force constant:

$$k_{ijk}^{BB} = \left(\frac{\left|\vec{R}_{ij}(n)\right|}{3E_{ij}I_{ij}} + \frac{\left|\vec{R}_{ik}(n)\right|}{3E_{ik}I_{ik}} \right)^{-1} . \tag{2.13}$$

The reason for using an overall constant, instead of one for each beam, is that the latter case would lead to *two two-body* potential terms, one for each beam. As a result, this cannot describe any rotations of the total *ijk* system, and $\Delta\theta_{ijk}^{ij}$ and $\Delta\theta_{ijk}^{ik}$ are considered independently.

The change in torsion angle $\Phi_{ijkl}(n)$ is defined as the total change of torsion angle of bond *ik* at increment *n*, relative to the initial torsion angle [i.e., $\Phi_{ijkl}(0) \equiv 0$]. It is the angle between (the projection of bond *ij* on a plane with normal in the direction of bond *ik*) and (the projection of bond *kl* on the same plane). This angle enters quadratically into the torsion (*T*) potential (Figure 2.4):

$$U_T(n+1) = \frac{1}{2}\sum_{<ijkl>} k_{ijkl}^T \Phi_{ijkl}^2(n+1) = \frac{1}{2}\sum_{<ijkl>} k_{ijkl}^T [\Delta\Phi_{ijkl}(n+1) + \Phi_{ijkl}(n)]^2, \tag{2.14}$$

where $\Delta\Phi_{ijkl}(n+1) \equiv \Phi_{ijkl}(n+1) - \Phi_{ijkl}(n)$ is the torsion angle increment. From elasticity theory,[10] the force constant (*T-constant*) between nodes *i*, *j*, *k*, and *l* is given by (where ν is Poisson's ratio):

$$k_{ijkl}^T = \frac{E_{ik}I_{ik}}{(1+\nu)\left|\vec{R}_{ik}(n)\right|}. \tag{2.15}$$

The summation in (2.14) is over all quadruplets <*ijkl*> of spheres with (spheres *j* and *k* within C_0 of sphere *i*) and (sphere *l* within C_0 of sphere *k*). The problem can effectively be reduced to the three-body problem by projecting bonds *ij* and *kl* onto the plane normal to bond *ik*. Defining

$$\vec{r}_{kl}(n) \equiv \vec{R}_{kl}(n) - [\vec{R}_{kl}(n) \cdot \hat{R}_{ik}(n)]\hat{R}_{ik}(n), \tag{2.16}$$

$$\vec{r}_{ij}(n) \equiv \vec{R}_{ij}(n) - [\vec{R}_{ij}(n) \cdot \hat{R}_{ik}(n)]\hat{R}_{ik}(n) \tag{2.17}$$

and proceeding with $\vec{r}_{ij}(n)$ and $\vec{r}_{kl}(n)$ as in the *BB* case, $\Delta\Phi_{ijkl}(n+1)$ can be written as

$$\begin{aligned}\Delta\Phi_{ijkl}(n+1) &= \Delta\vec{u}_{ij}(n+1).\left(\frac{\hat{R}_{ij}(n)\times\hat{R}_{ik}(n)}{\left|\vec{R}_{ij}(n)\right|\{1-[\hat{R}_{ij}(n)\times\hat{R}_{ik}(n)]^2\}}\right)+ \\ &\Delta\vec{u}_{kl}(n+1).\left(\frac{\hat{R}_{kl}(n)\times\hat{R}_{ik}(n)}{\left|\vec{R}_{kl}(n)\right|\{1-[\hat{R}_{kl}(n)\times\hat{R}_{ik}(n)]^2\}}\right) \\ &\equiv \Delta\vec{u}_{ij}(n+1)\cdot\vec{T}_j + \Delta\vec{u}_{kl}(n+1)\cdot\vec{T}_l.\end{aligned} \tag{2.18}$$

The angle change $\Phi_{ijkl}(n)$ is given by

$$\Phi_{ijkl}(n) = \cos^{-1}[\hat{r}_{kl}(n)\cdot\hat{r}_{ij}(n)] - \cos^{-1}[\hat{r}_{kl}(0)\cdot\hat{r}_{ij}(0)]. \tag{2.19}$$

In the expression for U_{CF} [Eq. (2.2)] the $\left[\left|\vec{R}_{ij}(n)\right| - \left|\vec{R}_{ij}(0)\right|\right]$ term is a constant for increment (n+1). It represents the central force between spheres i and j already present at the beginning of increment (n+1). The same holds for the $\theta_{ijk}(n)$ term in the three-body case and the $\Phi_{ijk}(n)$ term in the four-body case. In other words, the system is not relaxed or stress free before the next increment. The force $F_\alpha^q[N]$ on sphere α in the q direction consists therefore of two contributions:

$$F_\alpha^q(n+1) = [F_\alpha^q(n+1) - F_\alpha^q(n)] + F_\alpha^q(n) \equiv \Delta F_\alpha^q(n+1) + F_\alpha^q(n) \tag{2.20}$$

Applying this to *one* <*ij*> pair in U_{CF} gives the *reaction* force increment on node *i*:

$$\Delta F_i^{CF,q}(n+1) = -\left(\frac{\partial U^{CF}(n+1)}{\partial q_i}\right) = -k_{ij}^{CF}[\Delta\vec{u}_{ij}(n+1)\cdot\hat{R}_{ij}(n)]\hat{R}_{ij}^q(n) \tag{2.21}$$

The contributions of all <*ij*> pairs are added into a global stiffness matrix relating the displacements in the three coordinate directions of all spheres to all force increments in these directions. The same procedure is applied to the *BB*

and T contributions. When all entries are added into the global matrix, a system of (three times the number of spheres) linear equations is formed, or

$$\Delta\vec{F}(n+1) = [K]\Delta\vec{u}(n+1), \tag{2.22}$$

where $\Delta\vec{F}(n+1)$ is a $3N$-dimensional vector of the applied force *increments* at iteration step n, $[K]$ the $3N \times 3N$ stiffness matrix and $\Delta\vec{u}(n+1)$ $3N$-dimensional vector of the displacement increments at iteration n. Indeed, normally when torsional forces are included in the force balance the number of the equations to be solved for a 3D system of N nodes (or spheres) is 6N (three for the displacements and three for the rotations). The 3N case would be possible only if the torsional interactions are related, as stated above, to the displacements of actually a three-body bond-bending potential.

The external force is applied through the force vector. The resulting displacement increments are formally found from

$$\Delta\vec{u}(n+1) = [K]^{-1}\Delta\vec{F}(n+1), \tag{2.23}$$

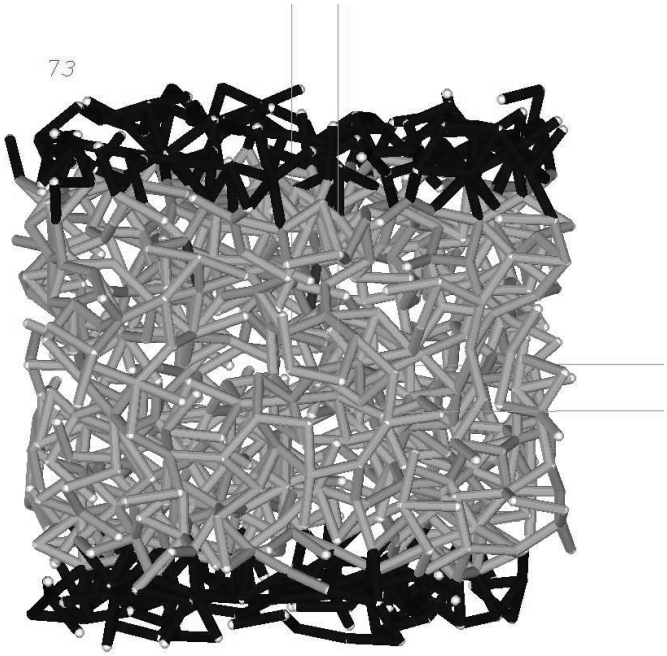

Figure 2.5. Intermediate stage in the fracturing process. Red bonds fulfill a fracture criterion.

but are actually obtained by solving the system of equations using a preconditioned conjugate gradient algorithm[11] which exploits the fact that [*K*] is a sparse matrix. Note that the $\Delta\vec{F}(n)$ terms do not explicitly enter this equation. The new positions at the end of increment *n*+1 are updated according to $\vec{r}_i(n+1) = \vec{r}_i(n) + \Delta\vec{u}_i(n+1)$.

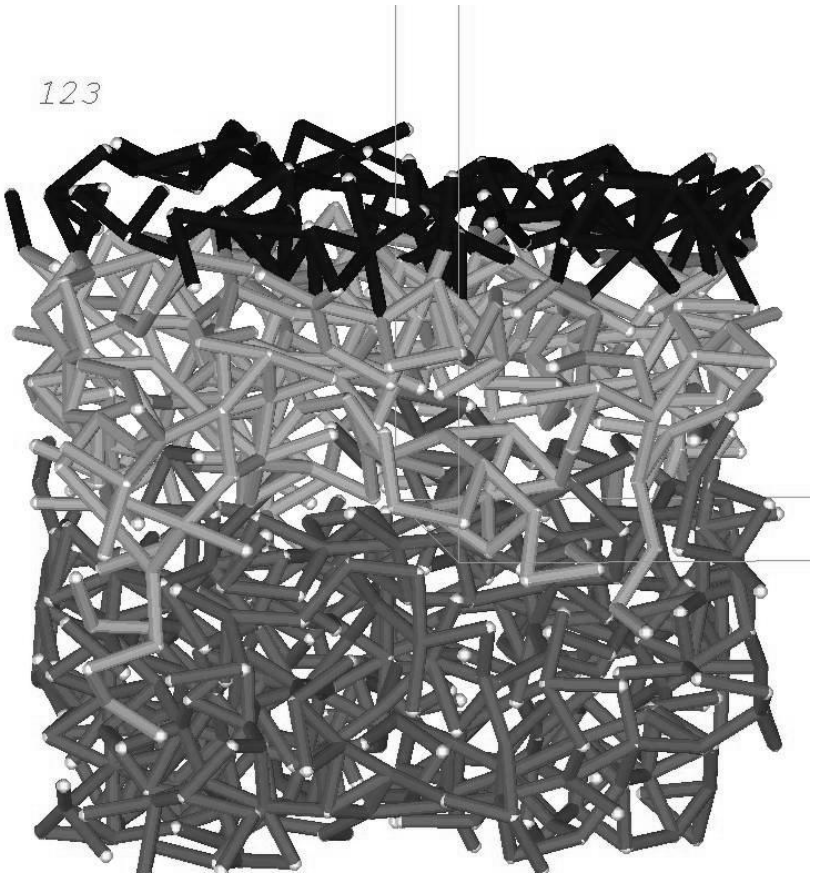

Figure 2.6: Final stage of fracture; the upper part is disconnected from the lower part

In Figure 2.5 an intermediate result is displayed and in Figure 2.6 the final configuration after complete failure is presented. The network has fallen apart into two separate parts, one of which is colored green.

2.3 DISCUSSION AND CONCLUSIONS

The geometrical disorder of highly porous brittle materials can be modeled using a three-dimensional disordered spring network. Some authors[1] use a

Hookean spring, or *central force (CF)*, potential. This is a two-body potential, which takes into account that the force exerted by a spring is linearly proportional to the displacement in the *axial* direction of the bond.

Others[2,4,5,7] include a three-body, or *bond-bending (BB)* term to account for the change in bond angle between neighboring bonds. The restoring force is proportional to the change in the bond angle. When bending of collinear bonds is not allowed, then the model is called the Kirkwood-Keating (KK) model. The reason for this is that for $\vec{R}_{ij}(n)$ parallel to $\vec{R}_{ik}(n)$, there is no unique plane defined by $\vec{R}_{ij}(n)$ and $\vec{R}_{ik}(n)$. The components $\Delta u_{ijk}^{ij}(n+1)$ and $\Delta u_{ijk}^{ik}(n+1)$ are only constrained by being normal to $\vec{R}_{ij}(n)$ and $\vec{R}_{ik}(n)$, respectively.[6]

To our knowledge, only one author has so far suggested that for 3D models a torsion term, i.e. a four-body potential, should be included.[6] At present, actual application in an elastic spring network has not been found in the literature. In this work, however, two-, three- and four-body interactions are included. In the four-body potential, a similar problem as in the three-body case arises for (almost) parallel bonds. When bond *ij* (or *kl*) is almost parallel to bond *ik*, $\left|\vec{r}_{ij}\right|$ (or $\left|\vec{r}_{kl}\right|$) can be small enough to invalidate the approximation $\Phi_{ijkl}^{ijk} \approx \tan \Phi_{ijkl}^{ijk}$. This can be circumvented by the following line of reasoning for the *ij* case: if $\left|\vec{r}_{ij}\right|$ is very small, the force needed to change the torsion angle significantly is very large. Also, when this is the case, the bonds are almost collinear. In that case, it is a reasonable approximation to regard bonds *ij* and *ik* as one single bond and apply the torsion potential to bonds $(ij + ik \equiv jk)$, *kl* and *jm*, where sphere *m* is a neighbor of sphere *j*. If sphere *j* does not have any neighbors (except for sphere *i*), then $\Delta\vec{u}_{ij}$ would be zero anyway, and $\Delta\Phi_{ijkl}$ would always be zero. The equation for $\Delta\theta_{ijkl}$ is now obtained simply by replacing each index *j* by *m* and each index *i* by *j*, with $\vec{R}_{jk} \equiv \vec{R}_{ji} + \vec{R}_{ik}$. The case that bond *kl* is almost parallel to *ik* is treated in the same way.

The indeterminacy arising in the bond bending case for parallel $\vec{R}_{ij}$ and $\vec{R}_{kl}$ does not arise in the torsion potential, since $\vec{R}_{ik}$ defines the plane into which the movement takes place. This does not hold if all three bonds are parallel, but that case can be circumvented in the way described previously.

It is important to note that the approach here presumes a more or less direct relationship between the spring network model and the microstructure of the porous material. Indeed, the elastic properties of the network, in terms of the spring constants $k_{ij}^{CF}, k_{ijk}^{BB}, k_{ijkl}^{T}$, are determined from the elastic properties of the matrix material, and from the geometry of the struts in the foam structure. This is distinctly different from most other approaches in the literature, where the spheres or nodes are usually arranged on a *regular* underlying lattice, e.g., square[2,3] or triangular[1] in two dimensions, or simple or body-centered cubic (bcc),[4-7] or hexagonal[1] in three dimensions. There, geometrical disorder is introduced by removing a number of bonds from the lattice according to some predefined probability distribution. The disordered network is considered to reflect a heterogeneous material, but without furnishing or assuming a relation with any actual material microstructure.

The model presented in this chapter lends itself well for research on the influence of size effects and of pore size distribution on the fracture process. Van den Born *et al.* [1] and Arbabi and Sahimi[5] were among the first to model compressive instead of tensile tests. This approach is also followed in this work. In the network representation of the porous microstructure, excluded volume effects have so far been neglected. Experimentally, however, some compaction of top and bottom surfaces takes place at the beginning of the fracturing process. Spheres that got disconnected after bond failure may in certain configurations still transmit some load. The present network representation lends itself for inclusion of an additional potential term reflecting this.

Networks of the type considered here, with central force as well as bending and torsion interactions between nodes, can also be treated by other methods. In particular, such networks are completely similar to what are termed 'frameworks' in structural engineering. In that case, neighboring nodes are connected by a beam as a structural element. Bending and torsion are then incorporated by individual beams between two nodes, rather than by strings of three and four nodes, respectively, as in the present approach.[3] This requires that each node not only has three displacements as degrees of freedom but also an orientation, measured by an additional three parameters (e.g., Euler angles). Thus, the geometric networks considered here can also be analyzed by

computational structural mechanics techniques, especially the finite element method.[12,13] The important difference with the present approach from a computational point of view, is that these finite element methods involve a more efficient method to incorporate bending and torsion, but the number of degrees of freedom in a given network is twice as large as in the present approach, where one has to solve three equations for each node.

The methodology has been tested for networks consisting of up to 8000 nodes on a SGI Power Indigo,[2] a 75 MHz R8000 workstation with 256 Mbytes of RAM. In order to give an indication of the CPU time involved: the sample case presented in Figure 2.5 and Figure 2.6 (1000 spheres, 2701 bonds) needed 136 relaxation steps for complete failure (973 bonds broken) in 86 seconds CPU time for each relaxation step (stopping criterion for each relaxation step: $\left|[K]\Delta\vec{u} - \Delta\vec{F}\right| / \left|\Delta\vec{F}\right| < \delta$, where $\delta = 10^{-10}$). This depends very sensitively on the average number of bonds per node, because the four-body potential term is a third nearest neighbor term. This number is strongly dependent on parameters in the configuration generation phase, such as the connectivity threshold C_0 (which is chosen to be as close to the bond percolation threshold as possible), and the parameters used in the Lennard-Jones potential. The sparse matrix solver used has not yet been optimized for computational speed however, since the main purpose of this work is to show that the proposed methodology actually leads to global failure of the network. Chapter 4 will contain a more quantitative study of the network properties, notably the scaling properties of the ultimate strength as a function of the network size.

2.4 References

[1] I.C. van den Born, A. Santen, H.D. Hoekstra, and J. Th. M. De Hosson, in *Fracture Processes in Concrete, Rock and Ceramics*, edited by J.J.M. van Mier, J.G. Rots, and A. Bakker (E & FN SPON, London, 1991), p. 231.

[2] S. Feng, P.N. Sen, B.I. Halperin, and C.J. Lobb, Phys. Rev. B 30, 5386 (1984) .

[3] H.J. Hermann, A. Hansen, and S. Roux, Phys. Rev. B 39, 637 (1989).

[4] M. Sahimi and S. Arbabi, Phys. Rev. B 47, 695 (1993).

[5] S. Arbabi and M. Sahimi, Phys. Rev. B 38, 7173 (1988).

[6] J. Wang, J. Phys. A 22, L291 (1989).

[7] S. Arbabi and M. Sahimi, Phys. Rev. B 23, 2211 (1990).

[8] I.C. van den Born, A. Santen, H.D. Hoekstra, and J.Th.M. De Hosson, Phys. Rev. B 43, 3794 (1991).

[9] M.P. Allen and D.J. Tildesley, *Computer Simulation of Liquids* (Oxford University Press, Oxford, 1992).

[10] S.P. Timoshenko, J.N. Goodier, *Theory of Elasticity*, 3rd ed. (McGraw-Hill, New York, 1982).

[11] A. van der Ploeg, Ph.D. Thesis, University of Groningen (1994).

[12] Y. Kantor and I. Webman, Phys. Rev. Lett. 52, 1891 (1984).

[13] T.J.R. Hughes, *The Finite Element Method* (Prentice-Hall, Englewood Cliffs, NJ, 1987).